# Mixing assisted direct formation of isotactic poly(1-butene) form I′ crystals from blend melt of isotactic poly(1-butene)/polypropylene

Youxin Ji, Fengmei Su, Kunpeng Cui, Ningdong Huang*, Zeming Qi, Liangbin Li*

*National Synchrotron Radiation Lab and College of Nuclear Science and Technology, CAS Key Laboratory of Soft Matter Chemistry, University of Science and Technology of China, Hefei, China*
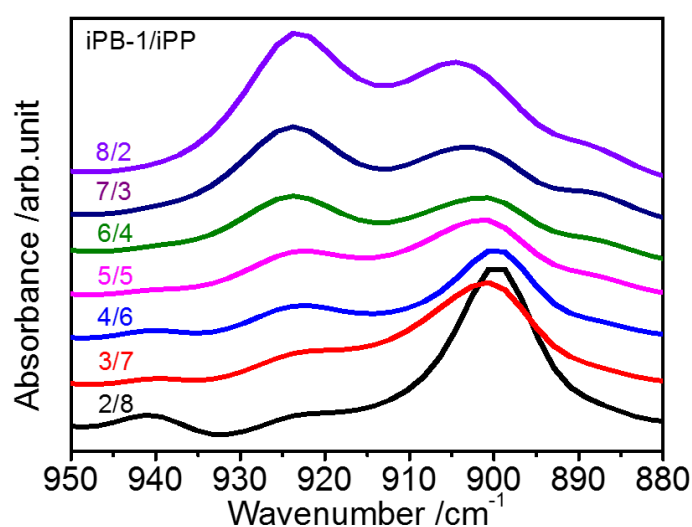
Figure S1. FTIR spectra of samples with different compositions quenched to 0 °C after annealing at 200 °C for 60 min.
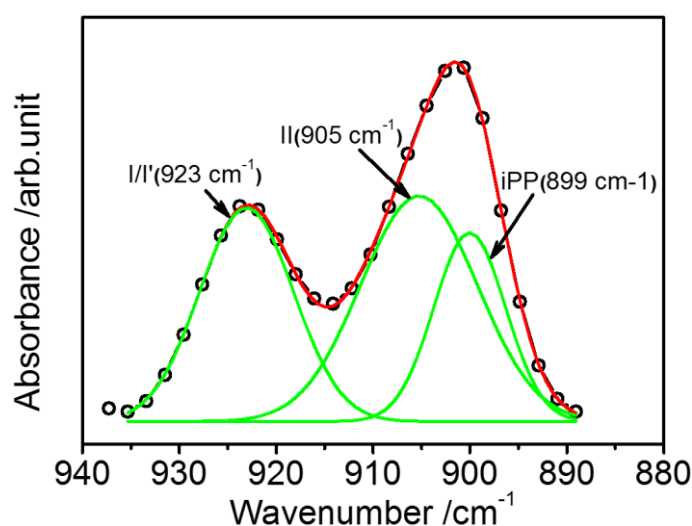


Figure S2. An example of peak fitting for FTIR spectrogram by Origin software. The value of integrated peak areas are obtained directly from the software after fitting.

---

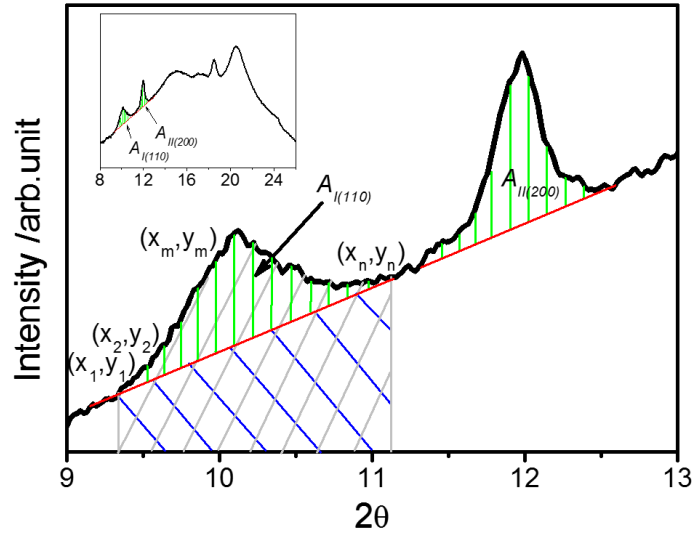* correspondence authors: ndhuang@ustc.edu.cn, lbli@ustc.edu.cn

Figure S3. Schematic diagram of simplified $A_{I(110)}$ and $A_{II(200)}$.

Take I/I'(110) peak as an example, the integral peak area $A_{I(110)}$ is obtained by subtract area of the blur region from that of the grey one. Thus, $A_{I(110)}$ can be approximate calculated by this equation:

$$A_{I(110)} = \left[\frac{1}{2}(y_1 + y_n) + (y_2 + y_{n-1})\right] * (x_2 - x_1) - \frac{1}{2}(y_1 + y_n) * (x_n - x_1) \quad (S1),$$

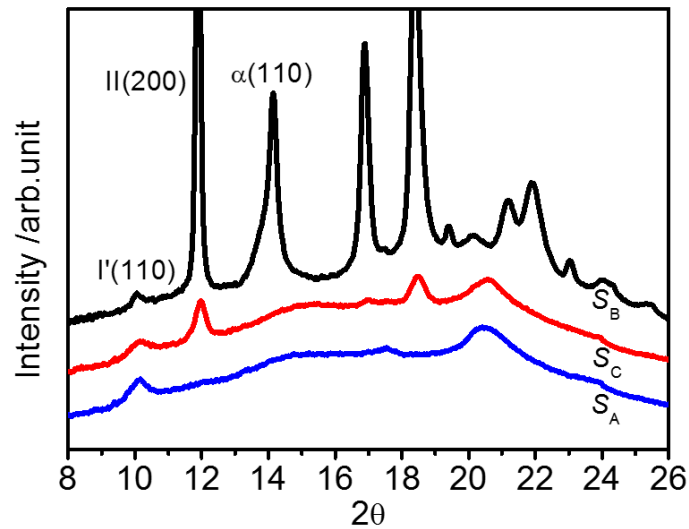where $(x_1,y_1),(x_2,y_2)\cdots(x_n,y_n)$ are the data points on the integrated 1D diffraction profile.



Figure S4. The integrated 1D diffraction profiles of $S_A$, $S_B$ and $S_C$.
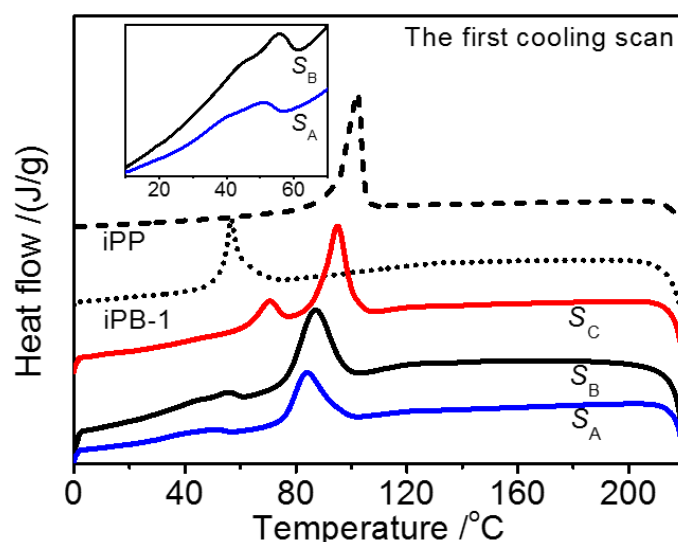
Figure S5. The DSC thermograms of the first heating scan of $S_A$, $S_B$, and $S_C$. The DSC thermograms of pure iPB-1 and iPP samples prepared with the same solution-precipitation method are also plotted for reference (The value of pure samples are multiplied by a constant to adjust to the same order of magnitude).

Table S1. Various parameters obtained from the DSC thermograms

| Sample ID | Thermal treatments | | $T_m$ (I′) (°C) | $T_m$ (II) (°C) | $T_m$ (I) (°C) | $T_m$ (iPP) (°C) | $\Delta H_m$ (I′) (J/g) | $\Delta H_m$ (II) (J/g) | $T_c$ (iPB-1) (°C) | $T_c$ (iPP) (°C) |
|---|---|---|---|---|---|---|---|---|---|---|
| | $Time_{anl}{}^a$ (min) | $T_Q{}^b$ or $T_C{}^c$ (°C) | | | | | | | | |
| $S_A$ | 120 | 0 | 89.5 | 106.3 | - | 141.2 | 7.5 | 1.9 | 50.9/40.1 | 83.7 |
| $S_B$ | 120 | 115 | 89 | 106.6 | - | 142.4 | 0.7 | 4.1 | 55.8/44.6 | 87.1 |
| $S_C$ | 10 | 0 | 90.5 | 110.9 | - | 144.1 | 2.0 | 6.2 | 70.6 | 95.0 |
| iPB-1 | - | - | - | 115.3 | 127.5 | - | - | - | 56.7 | - |
| iPP | - | - | - | - | - | 145.4 | - | - | - | 102.3 |

$^a$time persist at 220 °C. $^b$quenching temperature. $^c$isothermal crystallization temperature.

For samples with low degree of mixing (see $S_C$), the crystallization temperature $T_c$ reduces for iPP but increases for iPB-1 compared to the pure counterpart as shown in Table R1. Such changes can be rationalized by the following argument. In less mixing blend melts, the iPB-1 melt acts as a high viscosity polymeric diluent and reduces $T_c$(iPP) whereas the iPP crystalline phase acts as nucleating agent to increase $T_c$(iPB-1). On the other hand, for samples that two components are highly mixing or even miscible at molecule level with each other as in the case of $S_A$, $T_c$(iPP) and $T_c$(iPB-1) both decrease meaning suppression of the crystallization of both components. For miscible binary-melts, the potential energy of the system reduces,

resulting in a more stable thermodynamic state than that of homopolymer. Therefore, the nucleation barrier is increased and the nucleation ability decreases for both components in the blend. Meanwhile, the diffusing of crystallizable chain segments to the crystal growing front is reduced because of relative strong inter-molecular interactions between miscible molecular chains. For these reasons, the miscible parts of iPP and iPB-1 are more difficult to crystallize than the ordinary ones, resulting in the decrease of $T_c$ for both components. $T_c$(iPP) and $T_c$(iPB-1) show a larger extend of reduction for $S_A$ than for $S_B$, which can be attributed to the higher preserved mixing degree of the former than the latter before DSC cooling. It is speculated that in the sample preparation process the mixing degree of the $S_B$ decreases since the system go through a phase separation process and approaching to the co-existent compositions determined by this temperature during the long period of isothermal-crystallization at 115 $^{\circ}$C. As to $S_A$, iPP component crystalized or solidified first so quickly during fast quenching that littler iPP and PB-1 chains segregated before the crystallization of iPB-1 begins and the state of the blend melt may be relatively better preserved.

Furthermore, two weak exothermic peaks of iPB-1 can be perceived for $S_A$ and $S_B$ as shown by the magnified insert panel in Figure S5. Similar behavior has been observed in random ethylene/1-butene copolymers by Alamo et al.[1] They found that if melted in an intermediate temperature range, double-peaked exotherms or broader exotherms covering both nucleation regimes will appear. It has been explained by the existence of memory effect melt caused by the long crystallizable sequence partitioning in the melt. They concluded that two types of nucleation are present and one is nucleating from homogeneous melt, while the other comes from the heterogeneous melt with clusters constituted by the long crystallizable sequences. This explanation was also supported by Monte Carlo simulations performed by Hu et al.[2] Recently, a similar step-like crystallization behavior characterized by a double plateau upon cooling down the partially melted iPB-1 has been observed by Cavallo et al.[3] In our case, the two-step crystallization of iPB-1 is speculatively ascribed to the crystallization of the ordinary iPB-1 part and that assisted by the concentration fluctuations in the mixtures. The plausible two distinctive crystallization pathways, lead to the formation of form II and

form I′, respectively.

(1) Reid, B. O.; Vadlamudi, M.; Mamun, A.; Janani, H.; Gao, H. H.; Hu, W. B.; Alamo, R. G. *Macromolecules* **2013,** 46, (16), 6485-6497.

(2) Gao, H. H.; Vadlamudi, M.; Alamo, R. G.; Hu, W. B. *Macromolecules* **2013,** 46, (16), 6498-6506.

(3) Cavallo, D.; Gardella, L.; Portale, G.; Muller, A. J.; Alfonso, G. C. *Polymer* **2014,** 55, (1), 137-142.